

Carbon dioxide desorption from aqueous solutions of monoethanolamine and diethanolamine in a microchannel reactor

Babak Aghel^a, Sasan Sahraie^a, Ehsan Heidaryan^{b,c,*}

^a Department of Chemical Engineering, Faculty of Energy, Kermanshah University of Technology, Kermanshah, Iran

^b Department of Chemical Engineering, Engineering School, University of São Paulo (USP), Caixa Postal 61548, São Paulo, SP 05424-970, Brazil

^c Department of Chemical Engineering, Imperial College London, South Kensington Campus, London SW7 2AZ, United Kingdom

ARTICLE INFO

Keywords:
Desorption
Microchannel
Amine solvents
Mass transfer
Energy optimization

ABSTRACT

In this study, the process of carbon dioxide (CO_2) desorption from two saturated solutions of monoethanolamine (MEA) and diethanolamine (DEA) was performed in a microchannel made of stainless-steel grade 316 with a circular cross-section (diameter: 800 μm , length: 35 cm). The operating variables in this study were temperature (55, 75 and 95 °C), rich solvent flow rate (0.3, 0.9 and 1.5 ml/min), and inlet solvent concentration (10, 20 and 30 wt% of the amine). The mass transfer efficiency was determined based on the desorption percentage, volumetric liquid-side mass transfer coefficient (k_{Lav}), volumetric overall mass transfer flux (N_{CO_2av}), and energy consumption per unit mass CO_2 (R). The results showed that the use of a microchannel significantly increased the mass transfer rate and decreased energy consumption per removed CO_2 . The results also showed that the amount of k_{Lav} for the two solvents of MEA and DEA was 1.91 and 3.48 1/s, respectively. Moreover, the R -value for the two solvents of MEA and DEA was 1.3 and 1.63 MJ/kg CO_2 , respectively, which is at least three times lower than that of other mass transfer devices.

1. Introduction

Climate change is becoming a global concern. Greenhouse gases are regarded as the key cause of climate change. Carbon dioxide (CO_2) is one of the most important greenhouse gases [1–3]. Power plants are the main sources of CO_2 emissions [4,5]. Post-combustion carbon capture (PCC) is the most affordable way to reduce CO_2 emissions because it can be retrofitted to the existing power plants [6–8]. Various methods have been investigated to reduce CO_2 emissions, such as chemical/physical absorption, membrane, adsorption, and cryogenic distillation [9–13]. CO_2 absorption using alkanolamine solvents such as monoethanolamine (MEA), diethanolamine (DEA), and methyl diethanolamine (MDEA) is the most common and popular method for PCC [14–16]. However, these amine solvents require much energy for their regeneration. The regeneration energy accounts for about 70% of the total operation cost in PCC [17,18]. If a power plant is equipped with PCC, it will consume 25% to 40% of the energy generated in the power plant [19,20]. Therefore, it is essential to introduce new methods for reducing the energy requirements and thus, costs of PCC technology.

In general, there are two main ways to reduce CO_2 absorption costs: first, the introduction of new solvents with improved reaction kinetics

and second, the use of more efficient contactors to improve the mass transfer rate and thus reduce the equipment volume. Concerning the second strategy, one of the new technologies is the use of microchannels. Microchannels create a large surface area thereby increasing the absorption efficiency, and reduce the absorber size [21,22]. The absorption of CO_2 by amine solvents in microchannels has recently attracted the attention of researchers [23–26].

For energy savings, however, the desorption process is worth investigating further since it consumes about 70% of the total energy [27–29]. Therefore, optimization of the regeneration process in terms of mass and energy transfer plays an essential role in minimizing the energy and costs of PCC.

The desorption process is more complex because, in addition to mass transfer, heat transfer also plays a crucial role [30–34]. There are limited studies on the use of microchannels for CO_2 desorption. Nguyen et al. [35] studied the release of CO_2 in a microchannel with a diameter of smaller than 300 μm using surface waste heat. Liu et al. [36] experimentally examined the desorption of CO_2 from a rich methyl diethanolamine (MDEA) in a highly efficient microreactor, where the effects of MDEA concentration, desorption temperature, solvent velocity, and CO_2 loading on CO_2 desorption were studied. Nucleate boiling was

* Corresponding author at: Department of Chemical Engineering, Engineering School, University of São Paulo (USP), Caixa Postal 61548, São Paulo, SP 05424-970, Brazil.

E-mail address: heidaryan@engineer.com (E. Heidaryan).

Nomenclature	
α	Solution CO ₂ loading (mol CO ₂ /mol Amine)
a_V	Interfacial area per volume (m ² /m ³)
C	CO ₂ concentrations (mol/lit)
D_{CO_2}	Diffusion coefficient (m ² /h)
He	Henry coefficient
j_{CO_2}	Diffusion flux (kmol m ⁻² h ⁻¹)
$K_L a_V$	Overall mass transfer coefficient based on liquid phase (1/h)
$k_L a_V$	Volumetric liquid-side volumetric mass transfer coefficient (1/h)
l	Thickness of the liquid film (m)
M_{Amine}	Amine molecular weight (g/mol)
N_{CO_2}	Mass transfer flux (kmol m ⁻² h ⁻¹)
Q	Heat input (MJ)
q_L	Volumetric flow rate (l/h)
R	Desorption energy consumption (MJ/kg CO ₂)
T	Temperature (K)
V	Microchannel volume (m ³)
x_{CO_2}	Carbon dioxide molecular fraction in liquid phase (kmol/m ³)
x_{Amine}	Amine molecular fraction in solvent (kmol/m ³)
θ	The percentage of desorption (%)
Res	Response
β	Regression coefficients
X	Independent coded variables
DF	Degrees of freedom
MS	Mean squares
SS	Sum of squares
Subscripts	
g	Gas phase
L	Liquid phase
CO_2	Carbon dioxide
i	Interface
b	Bulk
in	Inlet
out	Outlet

considered as the dominant mechanism of heat transfer during the CO₂ desorption from the rich MDEA in the microchannel reactor [37]. However, Liu and colleagues' study was only conducted on one solvent type. They used a microreactor with a rectangular cross-section that caused a lack of uniformity in fluid temperature within the micro-reactor.

Today, MEA and DEA are mainly used in PCC due to their rapid reaction capability in CO₂ absorption. However, CO₂ desorption from these solvents has yet to be investigated in the microchannel. Therefore, it is necessary to conduct a comprehensive experimental study of mass transfer, heat transfer, and energy optimization in CO₂ desorption from amine solvents in a microreactor.

For this purpose, this study uses monoethanolamine (MEA) and diatolamidine (DEA) rich solvents. In this study, a stainless steel tube grade 316 with an internal diameter of 800 μm was used as the microchannel. Operating variables were desorption temperature, rich solvent flow rate, and solvent concentration. Moreover, the percentage of desorption, mass transfer flux, and coefficients were selected as the criteria for measuring the quality of the mass transfer. In the end, by examining the amount of energy consumed per removed CO₂, the quality of desorption in terms of energy consumption was assessed for these solvents, and it was compared with that of other mass transfer equipment.

2. Theory

2.1. Mass transfer

CO₂ desorption from a rich solvent follows the liquid-gas mass transfer mechanism. Several models have been proposed for analyzing the liquid-gas mass transfer. The two-film model is one of the most recognized models. In this model, the bulk liquid and gas phases have constant and measurable physical and chemical properties. A small part at the interface of the two phases has a concentration profile. This part is called a thin film. The concentration near the thin film is highly variable, and mass transfer often occurs at this interface. Resistance to the CO₂ mass transfer from the liquid phase to the gas phase includes two parts: resistance in the liquid phase and resistance in the gas phase.

The mass transfer rate (due to diffusion in the liquid phase) for CO₂ desorption from the solvent is calculated by the Fick's law [38]:

$$j_{CO_2} = D_{CO_2} \left(\frac{dx_{CO_2}}{dl} \right) \quad (1)$$

x_{CO_2}	Carbon dioxide molecular fraction in liquid phase (kmol/m ³)
x_{Amine}	Amine molecular fraction in solvent (kmol/m ³)
θ	The percentage of desorption (%)
Res	Response
β	Regression coefficients
X	Independent coded variables
DF	Degrees of freedom
MS	Mean squares
SS	Sum of squares
Subscripts	
g	Gas phase
L	Liquid phase
CO_2	Carbon dioxide
i	Interface
b	Bulk
in	Inlet
out	Outlet

where dl is the thickness of the liquid film. In practice, this equation has a major drawback: it is difficult to measure the thickness of the film and thus measure the two-phase surface area. Therefore, volumetric mass transfer flux is commonly used instead of mass transfer flux. The total volumetric mass transfer flux in the liquid phase is defined as follows:

$$N_{CO_2} a_V = K_L a_V (x_{b.CO_2} - x_{i.CO_2}) \quad (2)$$

Moreover, the total volumetric mass transfer flux in the liquid phase is obtained by [38]:

$$\frac{1}{K_L a_V} = \frac{1}{k_L a_V} + \frac{1}{He \cdot k_G a_V} \quad (3)$$

Since the liquid phase mass transfer dominates the total mass transfer [38,39], the following equation should be considered:

$$\frac{1}{K_L a_V} = \frac{1}{k_L a_V} \quad (4)$$

Therefore, the general equation of volumetric mass transfer flux is:

$$N_{CO_2} a_V = k_L a_V (x_{b.CO_2} - x_{i.CO_2}) \quad (5)$$

By considering the mass balance on the reactor volume, the volumetric mass transfer flux can be obtained by:

$$N_{CO_2} a_V = \frac{q_L x_{a \min e}}{V} (\alpha_{in} - \alpha_{out}) \quad (6)$$

By combining Eqs. (5) and (6), we reach the following:

$$N_{CO_2} a_V = k_L a_V (x_{b.CO_2} - x_{i.CO_2}) \quad (7a)$$

$$x_{i.CO_2} = 0 \quad (7b)$$

$$x_{b.CO_2} = x_{a_V.CO_2} \quad (7c)$$

$$x_{a_V.CO_2} = \frac{C}{M} \alpha_{a_V} \quad (7d)$$

$$k_L a_V = \frac{M_{Amine} q_L x_{a \min e}}{V C} \left(\frac{\alpha_{in} - \alpha_{out}}{\alpha_{a_V}} \right) \quad (7e)$$

$$\alpha_{a_V} = \frac{\alpha_{in} - \alpha_{out}}{\ln \left(\frac{\alpha_{in}}{\alpha_{out}} \right)} \quad (7f)$$

Finally, we reach the following equation to calculate the local mass transfer coefficient based on the liquid phase:

$$k_L a_V = \frac{M_{amine} q_L x_{a \min} e}{V C} \ln \left(\frac{\alpha_{in}}{\alpha_{out}} \right) \quad (8)$$

Furthermore, Eq. (9) shows the desorption percentage that is an important criterion for reaching an acceptable amine load for the absorption process. The higher the desorption percentage, the lower the amine load to absorb CO₂.

$$\theta = \frac{\alpha_{in} - \alpha_{out}}{\alpha_{in}} \times 100 \quad (9)$$

However, higher mass transfer rates do not always confirm higher desorption efficiency. It is necessary to apply higher temperatures to achieve a higher mass transfer rate in CO₂ desorption, but this will consume more energy. A validated criterion for measuring desorption efficiency is the calculation of energy consumption per the amount of CO₂ removed. Thus, according to Equation (10), R represents the regeneration energy (MJ/kg CO₂).

$$R = \frac{Q}{CO_2 \text{ desorption}} \quad (10)$$

The value of Q was measured using a power analyzer connected to the thermal element.

2.2. Chemistry

Several factors influence the rate of CO₂ desorption from aqueous alkanolamine solutions. One of the most important factors is the heat of the absorption reaction. Table 1 shows the physical properties of the two amines used in this study. Indeed, the heat of absorption reaction is the amount of heat released from the absorption reaction, which at a steady state conditions is equal to the amount of heat required for the desorption reaction. Therefore, with increasing the heat of absorption reaction, more energy is required to perform the desorption process. The increase in viscosity results in an increase in the amount of energy needed for desorption because it decreases heat transfer. As a result, the time to reach higher temperatures rises. Another critical factor is the solvent boiling point. The lower the boiling point of the solvent, the easier CO₂ in the solvent is removed at lower temperatures. Solvent vapor pressure is also an essential factor affecting the desorption rate. With increasing the solvent vapor pressure, the gas phase resistance increases more and, consequently, there is a decrease in the absorption rate [40–42].

CO₂ desorption efficiency depends on many operating variables, such as desorption temperature, reaction time, and solvent concentration. Therefore, this study considers three operating variables. The ranges of variables were determined based on the results of other similar studies and existing standards. To conduct a complete analysis the effects of these variables on the absorption efficiency, each of these variables was investigated at three levels. Due to the high significance of the solvent type, the effect of this variable with three other variables was studied. However, a similar experimental design was applied for each of the solvents. Accordingly, for each solvent, three operating variables at three different levels were investigated. These variables had the potential to be assessed using the response surface methodology (RSM) and experimental data. In this research, the Box-Behnken experimental design was used to determine the optimal conditions for maximizing the desorption efficiency [43–46]. The main operating variables were microchannel temperature (A), solvent flow rate (B),

Table 2
Operation parameters and their levels for desorption process.

Variables	Unit	Factors	Levels		
			+1	0	-1
Temperature	°C	A	95	75	55
Solvent flow rate	ml/min	B	1.5	0.9	0.3
Amine percentage in solvent	wt.%	C	30	20	10

Table 3
Operation responses for desorption process.

Responses	Notations	Unit	Equations
volumetric overall mass transfer flux	$N_{CO_2 a_V}$	kmol m ⁻³ h ⁻¹	(6)
volumetric liquid-side mass transfer coefficient	$k_L a_V$	1/s	(8)
CO ₂ desorption percentage	θ	%	(9)
desorption energy consumption	R	MJ/kg CO ₂	(10)

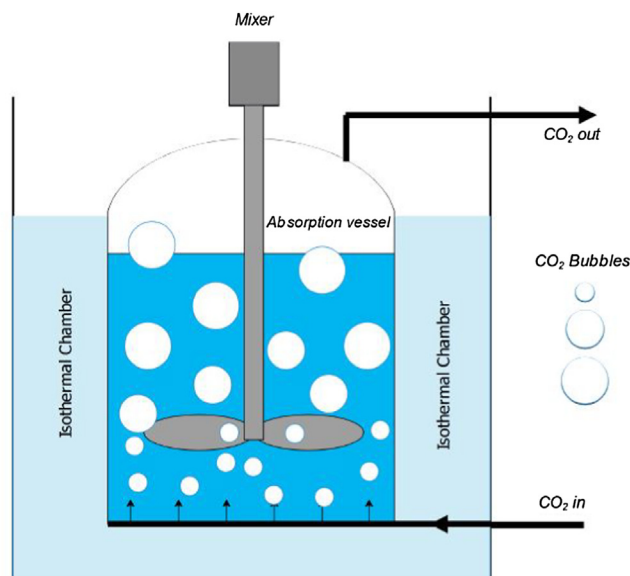


Fig. 1. Schematic of the system for loading of solvents with CO₂.

and amine percentage in solvent (C). The range considered for the operating variables and their levels is presented in Table 2. Another important variable is the CO₂ loading of the amine solvent entering the microchannel. Since MEA and DEA are the most commonly used amines in the industry, their CO₂ loadings entering the desorption unit is known, 0.48 and 0.50 mol CO₂ per mol solvent for MEA and DEA, respectively.

Analysis of Variance (ANOVA) is a precise method for analyzing and defining the degree of assurance of experimental data [47]. Statistical analysis of the model was performed by ANOVA. Using a quadratic model between Response (Res) and operating variables was fitted. The mathematical model is shown in the following equation:

Table 1
Physical properties of MEA and DEA.

Amines	Heat of reaction (MJ/kg CO ₂)	Viscosity @ 75 °C (cP)	Boiling point @ 1 atm (°C)	Vapor pressure @ 75 °C (Pa)	Heat of evaporation at 1 atm (kJ/kg)	Specific heat capacity @ 75 °C (kJ/kg K)
MEA	2	2.8	171	1333	826	22.6
DEA	1.5	29	270	64	670	21.2

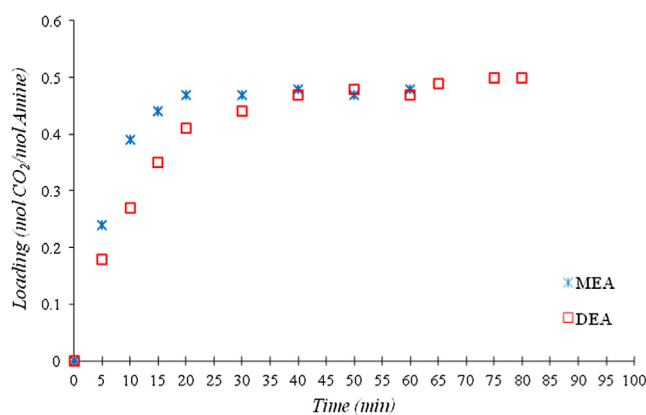


Fig. 2. The loading in aqueous alkylamine based absorbents.

$$Res = \beta_0 + \sum_{i=1}^3 \beta_i X_i + \sum_{i=1}^3 \beta_{ii} X_i^2 + \sum_{i=1}^2 \sum_{j=i+1}^3 \beta_{ij} X_{ij} \quad (11)$$

where X_i and X_{ij} are independent coded variables, β_0 is the intercept, and β_i , β_{ii} , and β_{ij} are regression coefficients. Table 3 presents responses, values of each, and the related methods of calculation.

The experimental mathematical model was tested by ANOVA with a confidence level of 5%. The F-value determines the statistical significance of the quadratic model. When the calculated F-value is greater than the F-value in the table, the P-value will be very small, indicating the significance of the statistical model. The calculated F-value is defined as the product of the division of the mean squares of the regression and the mean of the remaining squares:

$$F - value = \frac{MS_{regression}}{MS_{residual}} \quad (12)$$

where

$$MS_{regression} = \frac{SS_{regression}}{DF_{regression}} \quad (13)$$

$$MS_{residual} = \frac{SS_{residual}}{DF_{residual}} \quad (14)$$

The total degree of freedom (DF) is equal to the total number of experiments minus one. The degree of freedom of the regression is equal to the number of sentences minus one, and the degree of residual freedom is equal to the degree of total freedom minus the degree of freedom obtained from the regression analysis.

3. Experimental

3.1. Materials

CO_2 (99.5% purity) was purchased from the Faraman Oxygen Company, Kermanshah. Sulfuric acid ($\geq 98\%$), hydrochloric acid ($\geq 37\%$), Sodium sulfate ($\geq 99\%$) and Methyl orange indicator were purchased from Merck Company. MEA ($\geq 99\%$) and DEA ($\geq 98\%$) were purchased from Sigma-Aldrich. All chemicals were in analytical grade and used without further purification.

3.2. Apparatus and procedure

In this study, two devices were used. In the first step, the amine solvents were loaded with CO_2 by an apparatus (Fig. 1).

This procedure was carried out in a covered agitating container with a gas inlet at the bottom and a gas outlet on the top of it. The total volume of this container was 0.5 L, and it was filled with amine solvent up to 0.4 L. After filling the container with fresh solvent, the CO_2 inlet valve was opened, and the CO_2 was introduced into the container and mixed with the solvent. By entering the CO_2 gas into the solvent, part of the CO_2 was absorbed by the solvent and the rest left out via the outlet. Since the absorption is an exothermic therefore, by placing the container in a water bath the container temperature was maintained at ambient temperature. After CO_2 saturation, the MEA and DEA amines were loaded with 0.48 and 0.50 mol CO_2 per mol amines, respectively (Fig. 2). As presented in this Figure, the MEA saturation time is much shorter than that with the DEA due to the faster reaction rate of MEA with CO_2 .

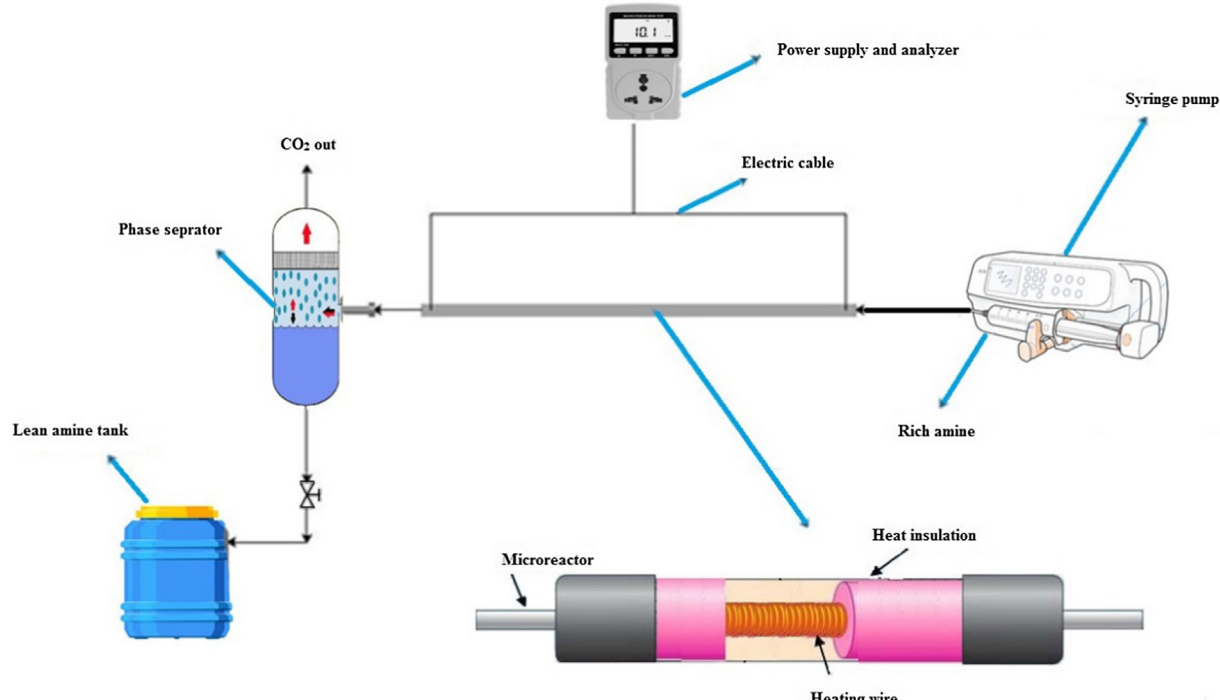
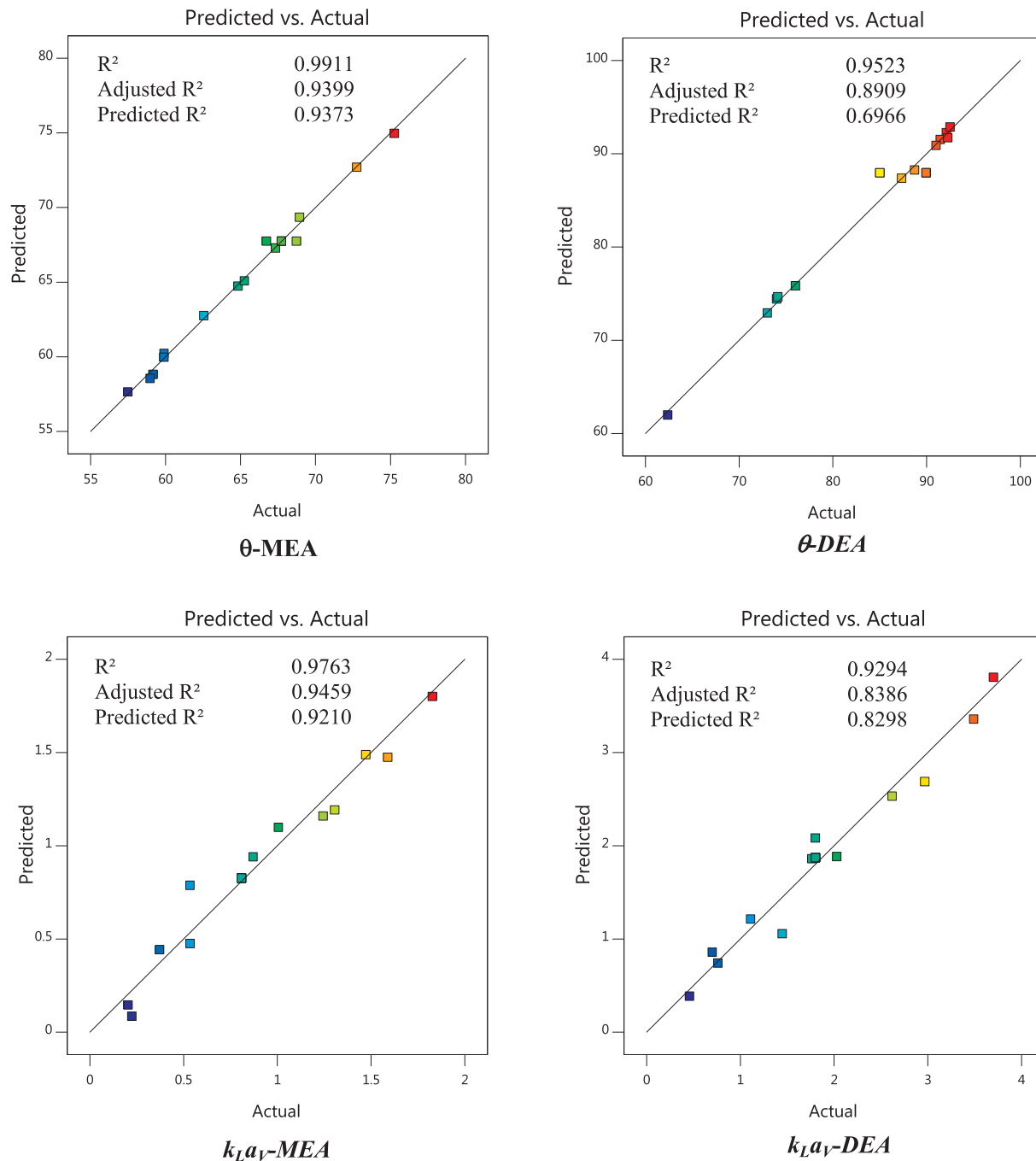


Fig. 3. Schematic of the desorption operation system.

Table 4

The quadratic mathematical model coefficients (based on coded variables).

	MEA, θ	DEA θ	MEA, $k_L a_V$	DEA, $k_L a_V$	MEA, $N_{CO_2} a_V$	DEA, $N_{CO_2} a_V$	MEA, R	DEA, R
Intercept	+ 67.75	+ 87.96	+ 0.8263	+ 1.87	+ 825.96	+ 1230.84	+ 1.97	+ 3.98
A	+ 4.40	+ 7.56	+ 0.3208	+ 0.4135	+ 274.22	+ 299.69	+ 1.41	+ 2.28
B	+ 0.8579	+ 0.6495	+ 0.5065	+ 1.07	+ 534.91	+ 721.53	+ 0.0189	+ 0.0690
C	- 1.70	- 7.88	+ 0.1949	+ 0.4020	+ 199.47	+ 128.70	- 1.60	- 2.35
AB	+ 1.45	+ 1.35	-	-	+ 134.39	+ 142.48	-	-
AC	+ 0.5668	+ 6.89	- 0.0540	-	-	+ 91.51	- 0.7783	- 1.56
BC	- 1.57	- 1.52	-	+ 0.4600	+ 76.17	-	-	-
A^2	+ 1.68	- 1.30	+ 0.1864	-	+ 81.72	-	+ 0.9571	+ 0.4859
B^2	- 6.79	- 3.95	- 0.0390	-	-	- 89.67	-	-
C^2	-	- 2.33	-	-	-	-	+ 1.09	+ 1.76

**Fig. 4.** Comparing the actual and predicted values of responses.

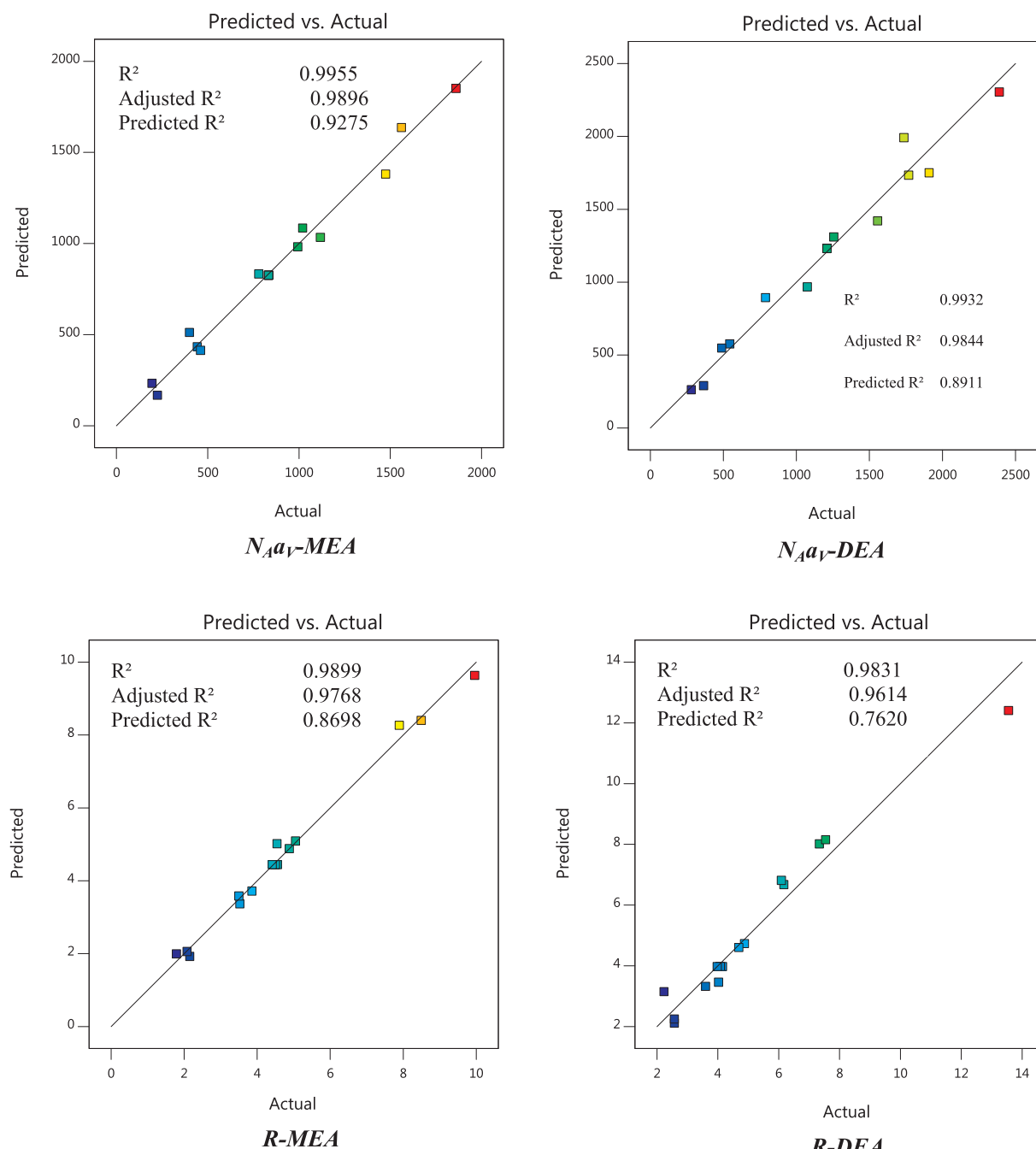


Fig. 4. (continued)

In the second step a new device was used to desorb CO_2 from the solvent (Fig. 3). This device had a stainless-steel tube with a diameter of 800 μm and a length of 35 cm, which was used as the microchannel. An electric heater coil around the microchannel was used to maintain the temperature. A dimmer and a power analyzer were installed to adjust the temperature and measure the power consumption of the heater. The stainless-steel tube and the coil were insulated to minimize the thermal loss. The rich amine was pumped into the microchannel by a syringe pump, and then CO_2 desorption occurred. The gas was released (major CO_2) from the upper part of a two-phase separator, and the lean amine (CO_2 -free) was released from the lower part of the separator. A titration method was used to analyze the CO_2 loading of the solvent. Using standard titration, this change in the solvent concentration was calculated, and its effect on the final loading was investigated.

4. Results and discussion

4.1. Analysis of variance of responses

A quadratic mathematical model using the least squares error method was obtained for each response, and the results are presented in Table 4. Table 4 presents the coded variables, and these equations represent the value of the response variable against the independent variables. The models were verified using backward analysis. As shown, all responses follow a quadratic polynomial model.

Using the Equations presented in above table, the model predicted the values of the responses and compared them with the observed values. The higher level of consistency between the observed and predicted values indicates the higher accuracy of the model. The comparisons between all the responses are shown in Fig. 4. The values of R^2 ,

Table 5
Standard deviation analysis (ANOVA) for quadratic model for θ .

Source	Sum of Squares	df	Mean Square	F-value	p-value	
MEA						
Model	405.50	8	50.69	146.32	< 0.0001	significant
A-Temperature	155.20	1	155.20	448.03	< 0.0001	
B-Solvent Flow Rate	5.89	1	5.89	17.00	0.0033	
C-Amine percentage in solvent	23.08	1	23.08	66.63	< 0.0001	
AB	8.37	1	8.37	24.16	0.0012	
AC	1.29	1	1.29	3.71	0.0903	
BC	9.85	1	9.85	28.43	0.0007	
A^2	11.87	1	11.87	34.25	0.0004	
B^2	194.68	1	194.68	561.99	< 0.0001	
Residual	2.77	8	0.3464			
Lack of Fit	0.7713	4	0.1928	0.3856	0.8107	not significant
Pure Error	2.00	4	0.5000			
Cor Total	408.27	16				
DEA						
Model	1268.66	9	140.96	32.23	< 0.0001	significant
A-Temperature	457.53	1	457.53	104.62	< 0.0001	
B-Solvent Flow Rate	3.38	1	3.38	0.7717	0.4088	
C-Amine percentage in solvent	496.58	1	496.58	113.54	< 0.0001	
AB	7.29	1	7.29	1.67	0.2378	
AC	190.11	1	190.11	43.47	0.0003	
BC	9.21	1	9.21	2.11	0.1899	
A^2	7.16	1	7.16	1.64	0.2413	
B^2	65.81	1	65.81	15.05	0.0061	
C^2	22.83	1	22.83	5.22	0.0562	
Residual	30.61	7	4.37			
Lack of Fit	1.32	3	0.4415	0.0603	0.9781	not significant
Pure Error	29.29	4	7.32			
Cor Total	1299.27	16				

Adjusted R² and Predicted R² for each response indicate the acceptable accuracy of the models.

The analysis of variance of the model for CO₂ desorption percentage responses is presented in Tables 5. A comparison between the tabulated F-value and the calculated F-value shows that all the models have a high level of significance (P < 0.0001).

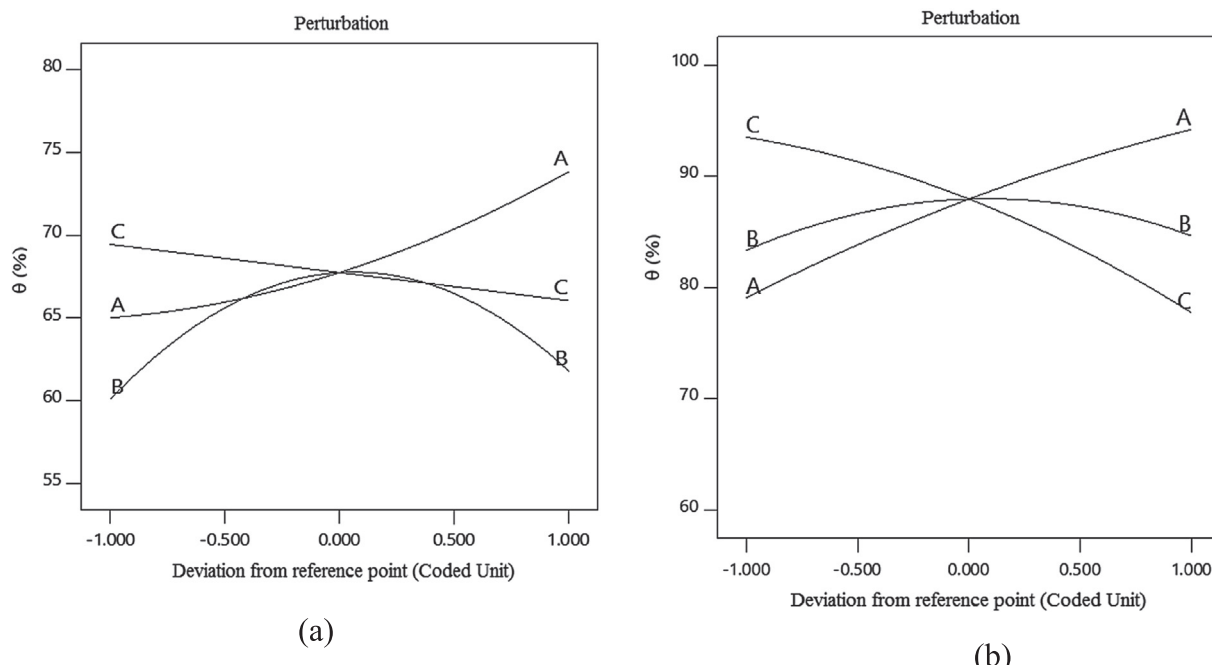
P values less than 0.05 show that model sentences are more significant. For example, the percentages of desorption by the MEA solvent are significant for variables A, B, C, AB, AC, BC, A^2 , and B^2 . P values more than 0.1 indicate that the regression sentences (such as C^2) are non significant. Insignificant sentences can be removed to make the model more accurate. Thus, non significant sentences were omitted from the quadratic model, and only significant sentences remained. The F-value of the non-fit was 0.3856, and therefore, the non-fit in proportion to the absolute error was non significant. The non significance of the non-fit is good because we want the model to fit the empirical data.

4.2. Analysis of responses

4.2.1. CO₂ desorption percentage (θ)

Temperature: increasing the temperature of the microchannel reduces the solubility of CO₂ in the solvent, which also increases the rate of desorption and, consequently, the percentage of desorption for the two solvents. Fig. 5 shows that with the increasing temperature, the percentage of desorption increased for the two solvents. A comparison of the increasing trends of desorption percentage of the two solvents shows that at lower temperatures (55–75 °C), the increasing trend in MEA solvent was lower than the DEA solvent; it might be attributed to the fact that the CO₂ desorption from primary amines generally requires a higher temperature. Accordingly, it can be seen that at higher temperatures (75–95 °C), the increasing trend of the desorption percentage has a steeper slope. This process is almost the opposite for the DEA solvent.

Solvent flow rate: Fig. 5 shows that in low flow rates (0.3–0.9 ml/min), the increase in solvent flow rate increases the desorption



A: Temperature (°C) B: Solvent Flow Rate (ml/min) C: Amine percentage in the solvent (wt.%)

Fig. 5. Perturbation plot for CO₂ desorption percentage from amine solutions (a) MEA, (b) DEA based on coded variables. A: Temperature (°C) B: Solvent Flow Rate (ml/min) C: Amine percentage in the solvent (wt.%).

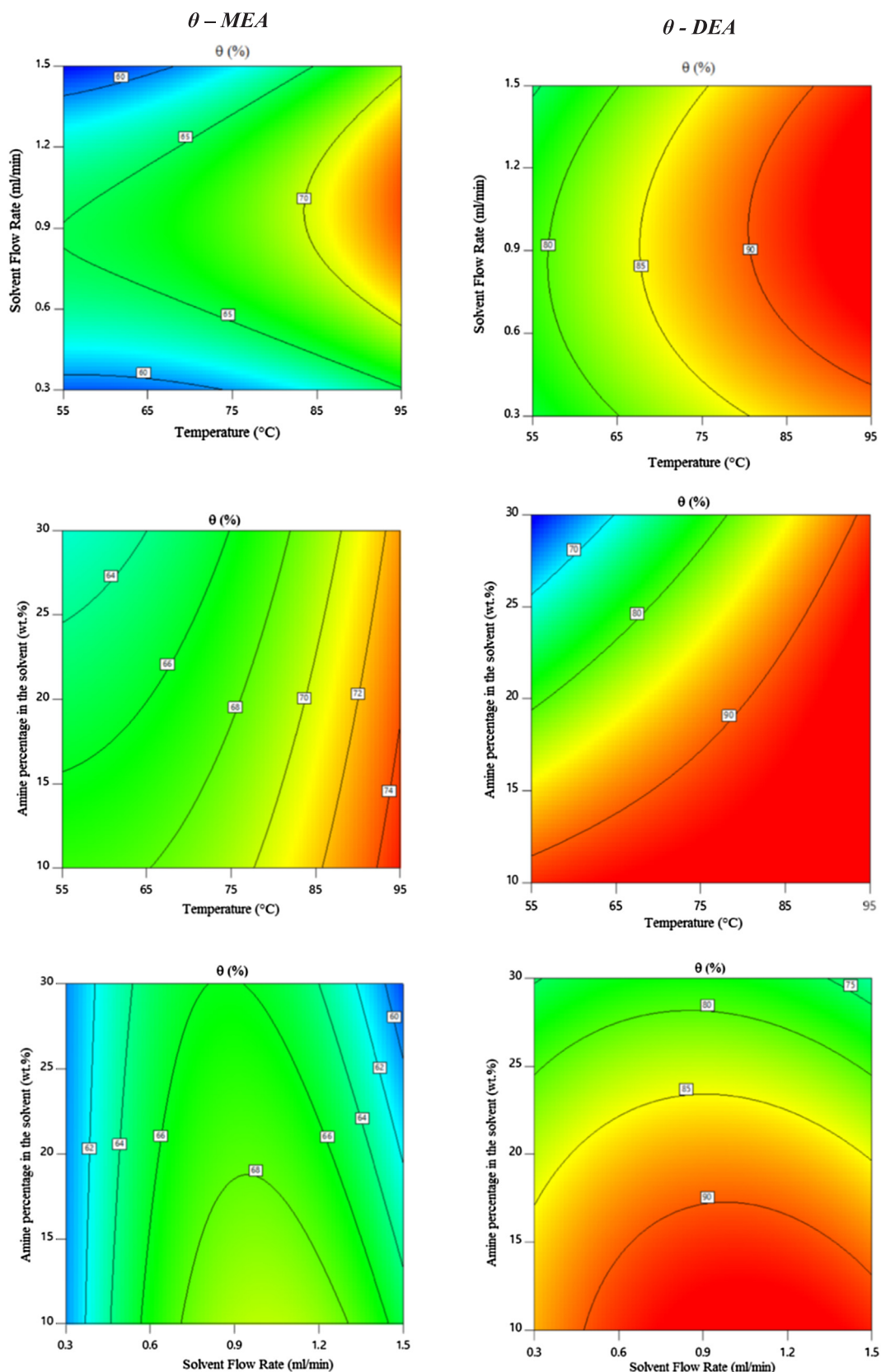
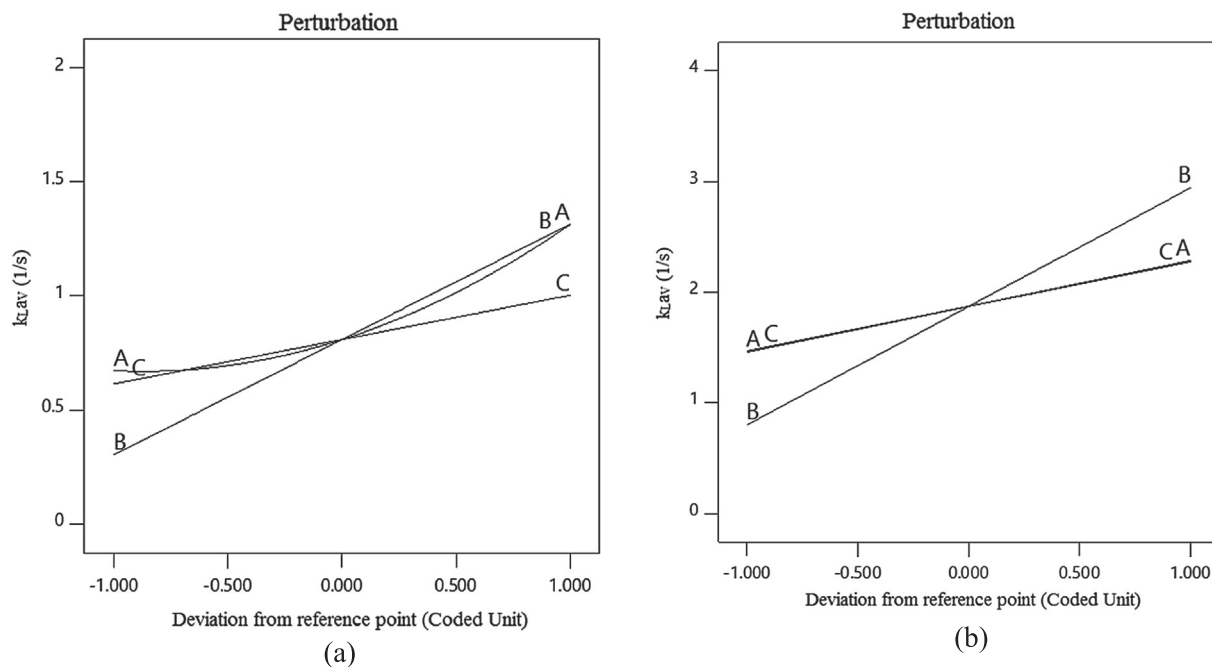
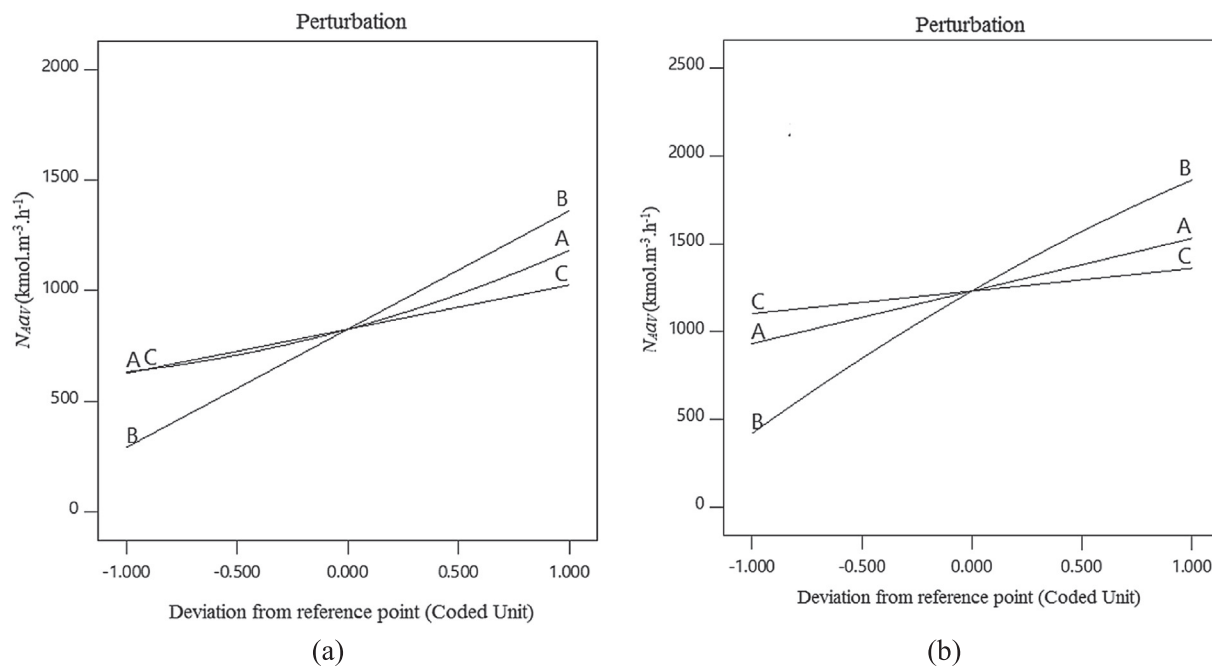


Fig. 6. Contour plots of CO_2 desorption percentage (θ) based on the actual temperature, solvent flow rate, and amine percentage in the solvent.



A: Temperature (°C) B: Solvent Flow Rate (ml/min) C: Amine percentage in the solvent (wt.%)

Fig. 7. Perturbation plot for volumetric liquid-side mass transfer coefficient from amine solutions (a) MEA, (b) DEA based on coded variables. A: Temperature (°C) B: Solvent Flow Rate (ml/min) C: Amine percentage in the solvent (wt.%).



A: Temperature (°C) B: Solvent Flow Rate (ml/min) C: Amine percentage in the solvent (wt.%)

Fig. 8. Perturbation plot for volumetric overall mass transfer flux from amine solutions (a) MEA, (b) DEA based on coded variables. A: Temperature (°C) B: Solvent Flow Rate (ml/min) C: Amine percentage in the solvent (wt.%).

percentage in the two solvents.

However, with further increase in the flow rate of the rich solvent, the desorption percentage starts decreasing. With the increase in the flow rate of the rich solvent, there is a reduction in residence time; consequently, it prevents the transfer of enough heat to all the segments of the solvent in the microchannel, which reduces the desorption percentage. However, passing rich solvent from the microchannel at high temperatures causes the formation of two-phase flow through the

transfer of CO₂ from the liquid phase to the gas phase. The high surface area between the two gas and liquid phases in the microchannel, even at high temperatures, also results in CO₂ absorption into the solvent. Therefore, the gas phase should be removed from the microchannel as soon as possible. The increase in the flow rate of rich solvent accelerates the exit of the gas phase and, consequently, decreases the poor amine load from the microchannel. Therefore, the increase in the flow rate of rich solvent both increases and decreases the absorption percentage.

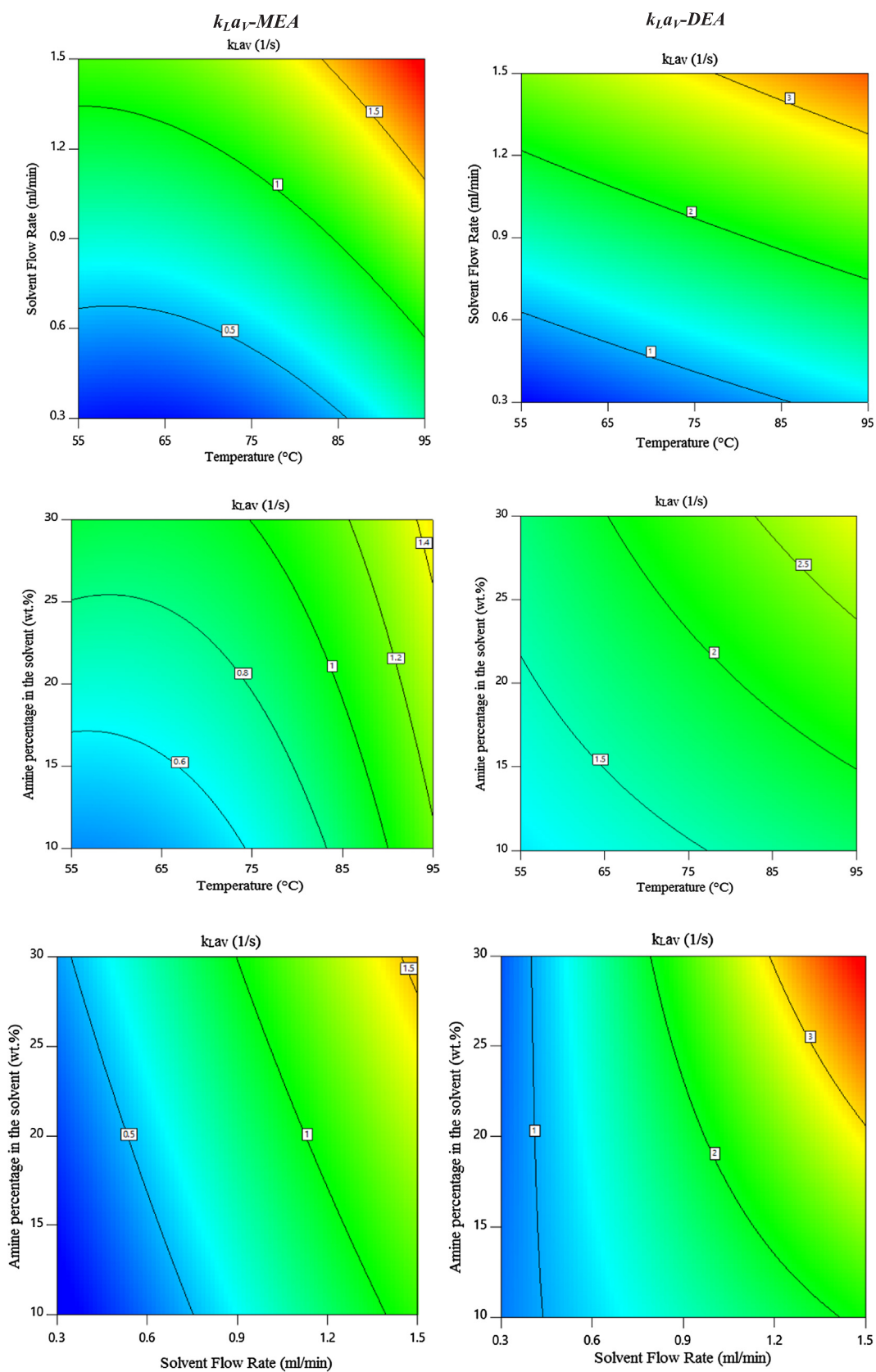


Fig. 9. Contour plots of volumetric liquid-side mass transfer coefficient ($k_L a_V$) based on the actual temperature, solvent flow rate, and amine percentage in solvent.

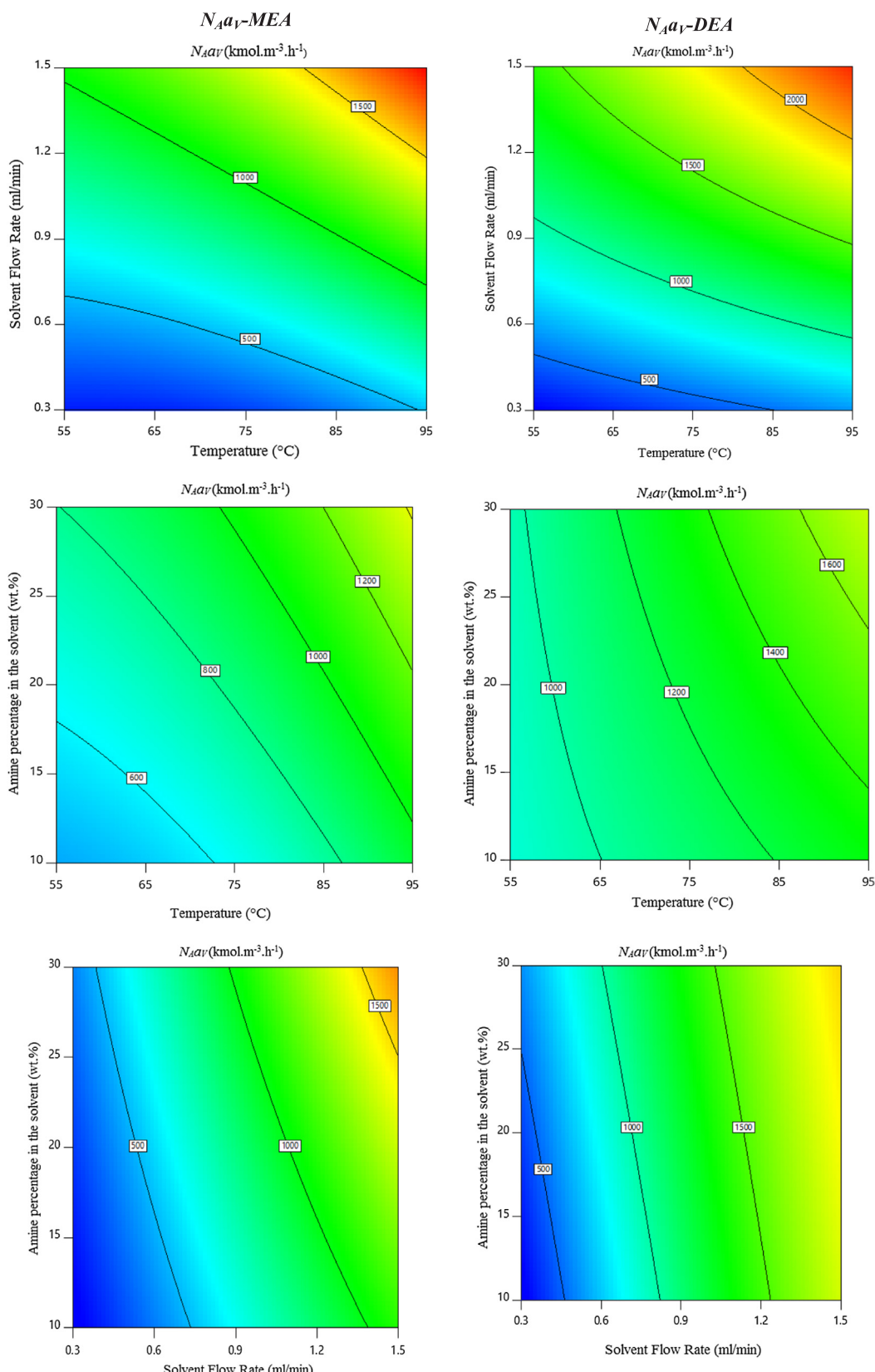


Fig. 10. Contour plots of volumetric overall mass transfer flux ($N_{CO_2} a_V$) based on the actual temperature, solvent flow rate, and amine percentage in the solvent.

Amine concentration in the solvent: On the one hand, the increase in amine concentration in the solvent results in an increase in the outlet amine load. In other words, the higher load of amine in the solvent induces more CO_2 to enter the microchannel and, consequently,

it increases its concentration in the output of the microchannel. By increasing the concentration of amine in the solvent, all these factors reduce the desorption percentage. On the other hand, the increase in the concentration of amine in the solvent increases the viscosity and

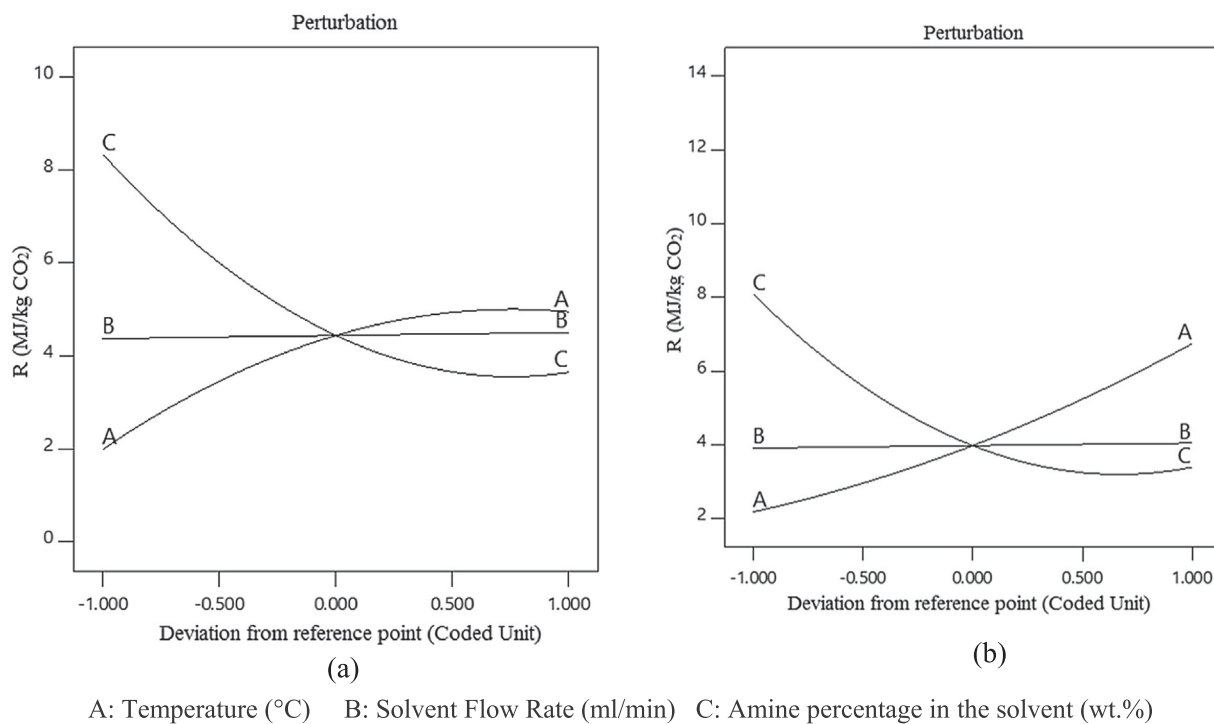


Fig. 11. Perturbation plots for desorption energy consumption (a) MEA, (b) DEA based on coded variables. A: Temperature (°C) B: Solvent Flow Rate (ml/min) C: Amine percentage in the solvent (wt.%).

solvent boiling point, they make it harder to reduce the loading.

Fig. 6 shows the interaction effects of operating variables on the desorption percentage in the form of a contour plot. Here, we discuss the contour plots of the inlet solvent flow rate-temperature for the two solvents.

As shown in Fig. 6, when using an average amount of solvent flow, with increasing microchannel temperature up to 85 °C, there is no change in the desorption percentage due to the greater strength of the CO₂ bond with MEA than the DEA solvent flow. Therefore, the MEA solvent flow needs higher temperatures to desorb CO₂. However, when using the DEA solvent flow rate, an average increase in the temperature results in an immediate increase in the desorption percentage. By considering the contour plot of the inlet solvent flow rate amine concentration for the two solvents, it can be concluded that when using low concentrations of amine in the solvent, at first, a maximum desorption percentage is reached, and then the desorption percentage begins to decrease. However, at higher concentrations, this maximum level is not observed and, in some cases at high concentrations, especially for DEA solvent, the desorption percentage is independent of the solvent flow rate. Fig. 6 presents the operating ranges in which the desorption percentage is maximized.

4.2.2. Volumetric liquid-side mass transfer coefficient (k_{Lav}) and volumetric overall mass transfer flux (N_{CO2av}):

Temperature: Figs. 7 and 8 show the general effects of the operating variables on k_{Lav} and N_{CO2av} . Based on the reasons stated in the previous section, the increase in temperature for the two solvents increases the absorption rate and, consequently, increases k_{Lav} and N_{CO2av} . As a general rule, the rate of CO₂ desorption from amine solutions is slower at lower temperatures than at higher temperatures. Accordingly, the amount of amine loading has a negative relationship with the temperature.

Solvent flow rate: As shown in Figs. 7 and 8, the increase in the flow rate of the two solvents significantly increases k_{Lav} and N_{CO2av} .

It can see that the increase in the solvent flow rate directly increases k_{Lav} and N_{CO2av} . However, the increase in the amount of flow rate and

the transition into two phases at high temperatures in the microchannel can considerably increase the surface area.

The increase in surface area causes a massive increase in mass transfer. Accordingly, the changes in k_{Lav} and N_{CO2av} against the changes in the flow rate of solvent are somehow linear and similar to Eqs. (6) and (8). However, the decrease in residence time and the increase in the outlet amine load somewhat decelerate the increase.

Amine concentration in the solvent: Eqs. (6) and (8) show that amines in the solvent directly affect k_{Lav} and N_{CO2av} ; it is also proved by Figs. 7 and 8.

Also, the concentration of amine in the solvent decreases the mass transfer by increasing the amount of amine load in the solvent. Generally, increasing the concentration of amine in the solvent increases viscosity, reaction heat, and boiling point of the solvent and, consequently, decrease the mass transfer. However, increasing the concentration of amine in the solvent causes a sharp increase in the number of CO₂ available for desorption, which is enough to increase the concentration of amine in the solvent and increase the mass transfer rate.

Figs. 9 and 10 present the contour plot of the effects of the operating variables on k_{Lav} and N_{CO2av} . The figures show that the highest values of k_{Lav} and N_{CO2av} for each of the two solvents were achieved at the maximum temperature and maximum solvent flow rate.

Fig. 9 shows that the increase in temperature at lower concentrations had a less significant effect on k_{Lav} .

4.2.3. Desorption energy consumption (R)

Temperature: The increase in temperature increases the mass transfer rate and, consequently, increases the amount of CO₂ desorbed from the solvent. However, applying higher temperatures also results in a higher level of energy consumption. Fig. 11 shows that, for MEA solvent, the increase in temperature initially increases the R -value but later, this incremental slope decreases slightly, and after reaching a constant value of R , the increase in temperature no longer affects the R -value. It might be attributed to the fact that increasing the temperature initially increases energy consumption without a significant increase in

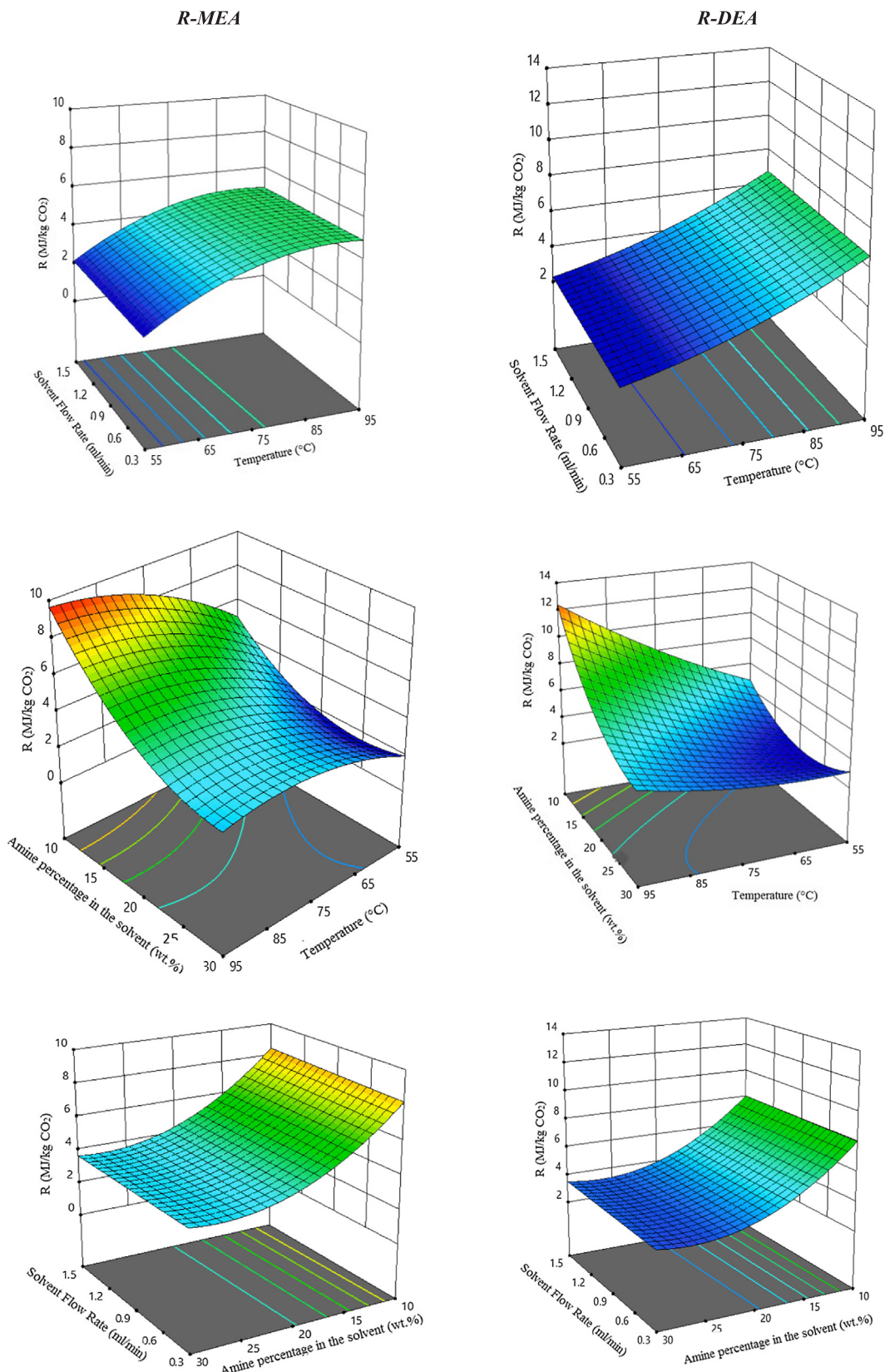


Fig. 12. Surface plots for desorption energy consumption (R) based on the actual temperature, solvent flow rate, and amine percentage in the solvent.

CO_2 desorption from the MEA solvent (due to the excessive demand of MEA for a high level of energy for desorption process). However, afterward, with the initiation of desorption from the solvent, the denominator of Eq. (10) also begins to increase and shifts the R -value

toward a constant value. This process is similarly performed for the DEA solvent, but there is a difference. Fig. 11, representing the DEA solvent, shows that at low temperatures, because of the weakness of the CO_2 binding to DEA, desorption process is not performed and with

Table 6

Optimum values of the process parameter for desorption process.

Solvent	θ (%)	k_{lA_V} (1/s)	N_{AA_V} ($\text{kmol m}^{-3} \text{h}^{-1}$) $\times 10^3$	R (MJ/kg CO_2)
MEA	75.55	1.91	2119	1.3
DEA	98.46	3.48	2338	1.63
Temperature (°C)	95	95	95	55
Solvent flow rate (ml/min)	0.9	1.5	1.5	0.9
Amine concentration (wt.%)	10	30	30	30

increasing the temperature (energy consumption), the R-value increases as well. However, since no CO_2 is left to be desorbed from the solvent, the increase in temperature directly increases the R-value.

Solvent flow rate: The increase in the solvent flow rate not only increases the desorption rate but also increases the energy consumption used to maintain operating temperature. These two factors neutralize the effects of each other and remove the sensitivity of the R-value to the solvent flow rate. Fig. 11 shows that the changes in the solvent flow rate in the two solvents does not have much effect on the R-value.

Amine concentration in the solvent: Fig. 11 shows that in the two solvents, the increase in the concentration of amine initially causes a significant reduction in the R-value. However, when the R-value reaches a specific value, it no longer decreases. The increase in the concentration of amine in the solvent not only increases the mass transfer and the desorption rate but also leads to changes in the physical properties of the solvent. One of the most important physical properties is the specific heat capacity of the solvent; when the thermal capacity is higher, the solvent resistance to the increased temperature is also higher. Table 1 shows the values of the specific heat of the MEA and DEA. Comparing these values with a specific heat capacity of water (4.187 at 75 °C (kJ / kg K)) proves that the increase in the amine concentration in the solvent leads to a reduction in the specific heat capacity of the solvent. Therefore, increasing the concentration of amine in the solvent reduces its specific heat capacity, which, in turn, reduces the amount of energy consumed and eventually reduces the R-value. Of course, an excessive increase in the concentration of the amine increases the solvent vapor pressure and the viscosity, and consequently reduces the desorption rate and increases energy consumption.

Fig. 12 shows the three-dimensional graph of the interaction between variables and their optimal operating range for obtaining the best R-values.

The figure shows the interaction between temperature-amine concentration in the MEA solvent. At low concentrations of the solvent, the increase in temperature significantly increases the R-value and, as a result, reduces the energy efficiency of the desorption process. However, at low concentrations of the solvent, the increase in temperature initially increases the R-value and then decreases it. This may be because at low concentrations of the solvent, due to its higher specific heat capacity, the increase in the temperature of the microchannel is mainly used to overcome the heat capacity of the solvent without increasing the solvent temperature. Nevertheless, in higher

concentrations of the solvent, due to reduced specific heat capacity of the solvent, the increase in microchannel temperature can lead to desorption.

4.3. Comparison of the two solvents in terms of the mass transfer and desorption energy

Comparison of the two solvents of MEA and DEA shows that the desorption rate in the DEA solvent is higher than that MEA solvents. The results of the optimization show that N_{AA_V} for the DEA solvent can reach the 2338×10^3 kmol/m.h in optimal operating conditions (Temperature: 95 °C, Solvent flow rate: 1.5 ml/min, Amine percentage in the solvent: 30 wt%). Under such a condition, k_{lA_V} can reach a significant value of 3.48 1/s. These values indicate that the use of a microchannel for desorption significantly reduces the size of the mass transfer device, which, in turn, significantly reduces the cost of building a unit. On the other hand, as shown in Table 6, after the optimization, the R-values for each of the two solvents is between 1.3 and 1.63 MJ/kg CO_2 . The lowest value was observed in the DEA solvent, and the highest value was related to the MEA solvent. These values are of great importance as in packed bed columns, this value ranges from 2.5 to 3.5 MJ/kg CO_2 [29,48,49]. Therefore, it can be concluded that the use of microchannels to desorb CO_2 from amine solutions reduces energy consumption by about 50%; it might be attributed to the fact that in microchannels, due to the high surface area, the mass transfer and heat is higher.

5. Conclusion

The study of the effects of operating variables on the CO_2 desorption from amine solutions showed that the increase in the desorption temperature (55–95 °C), the flow rate of inlet rich solvent (0.3–1.5 ml/min), and the concentration of the solvent (10–30 wt%) increased k_{lA_V} (until the 1.91 and 3.48 (1/s) for MEA and DEA, respectively) and N_{CO_2av} (until the 2119 and 2338 ($\text{kmol m}^{-3} \text{h}^{-1}$) for MEA and DEA, respectively). Among them, the changes in the rich solvent flow rate had the greatest impact on the values of liquid-side volumetric mass transfer coefficient and volumetric overall mass transfer flux. However, the results showed that the increase in temperature (55–95 °C) and the solvent concentration (10–30 wt%), respectively, increased and decreased CO_2 desorption percentage (until the 77.55 and 98.46 (%) for MEA and DEA, respectively). Furthermore, with increasing the flow rate of the rich solvent (0.3–1.5 ml/min), θ initially increased and then decreased. By considering the effect of operating variables on the desorption energy consumption, it can be concluded that the change in the solvent flow rate did not have a significant effect on this value. However, for the MEA solvent, the increase in the temperature initially increased the desorption energy consumption and then fixed it. For the DEA solvent, however, the desorption energy consumption changed in all the ranges of temperature. By comparing these two solvents in term of absorption efficiency, it was found that the DEA solvent was more efficient than the MEA solvent.

Nevertheless, the efficiency of a solvent can be fully confirmed only

Table 7

Comparison of desorption energy consumption values obtained in this study with other studies in the most optimal operating conditions.

Contactor	Geometry of contactor	Solvent	Temperature (°C)	R (MJ/kg CO_2)	Refrence
Packed column	0.028 m × 0.50 m (internal diameter × packed height)	MEA	90 (reboiler temperature)	4.25	[50]
	0.06 m × 1.0 m (internal diameter × packed height)	DETA	3.44		[50]
	0.107 m × 2.0 m (internal diameter × packed height)	MEA	110 (reboiler temperature)	4.39	[51]
	0.03 m × 0.60 m (internal diameter × packed height)	MDEA		2.03	[51]
Microreactor	0.007 m × 0.035 m (internal diameter × microreactor lenght)	MEA	115 (reboiler temperature)	3.88	[52]
		DEA		3.25	[53]
		MEA	55 (desorption temperature)	1.3	This work
		DEA		1.63	

when its absorption efficiency is compared with its deposition efficiency. However, it can be stated decisively that, as compared with other mass transfer devices, the use of a microchannel as a means for mass transfer for the two solvents improved the CO₂ desorption efficiency, both in terms of mass transfer rate and energy saving. Under the best condition, when using other mass transfer devices such as a packed bed column, the desorption energy consumption rarely becomes less than 2.5, while in this study, the desorption energy consumption for the two solvents was less than 1.63 and for MEA it reached 1.3 MJ/kg CO₂. Table 7 compares the desorption energy consumption values in the microreactor with the packed columns for several common amines.

Briefly, it can be stated:

1. This equipment has a high potential for industrialization considering the mass transfer coefficient and the mass transfer flux from amine solvents in the microreactor.
2. The optimization of the operating conditions of the desorption process to achieve the highest efficiency was first performed in the microreactor.
3. Two commonly used solvents (MEA, DEA) in the desorption process based on the required energy for desorption have been investigated.

Declaration of Competing Interest

The authors declare that they have no known competing financial interests or personal relationships that could have appeared to influence the work reported in this paper.

References

- [1] C.T. Molina, C. Bouallou, Assessment of different methods of CO₂ capture in post-combustion using ammonia as solvent, *J. Clean. Prod.* 103 (2015) 463–468.
- [2] R.K. Pachauri, M.R. Allen, V.R. Barros, J. Broome, W. Cramer, R. Christ, J.A. Church, L. Clarke, Q. Dahe, P. Dasgupta, Climate change 2014: synthesis report. Contribution of Working Groups I, II and III to the fifth assessment report of the Intergovernmental Panel on Climate Change, Ipc, 2014.
- [3] S. Toghayani, E. Afshari, E. Baniasadi, M.S. Shadloo, Energy and exergy analyses of a nanofluid based solar cooling and hydrogen production combined system, *Renew. Energy*. 141 (2019) 1013–1025.
- [4] M. Zhang, Y. Guo, Rate based modeling of absorption and regeneration for CO₂ capture by aqueous ammonia solution, *Appl. Energy*. 111 (2013) 142–152.
- [5] P. Chen, Y.X. Luo, P.W. Cai, CO₂ capture using monoethanolamine in a bubble-column scrubber, *Chem. Eng. Technol.* 38 (2015) 274–282.
- [6] G. Léonard, D. Toye, G. Heyen, Experimental study and kinetic model of monoethanolamine oxidative and thermal degradation for post-combustion CO₂ capture, *Int. J. Greenh. Gas Control*. 30 (2014) 171–178.
- [7] H. Winkler, R. Spalding-Fecher, L. Tyani, Comparing developing countries under potential carbon allocation schemes, *Clim. Policy*. 2 (2002) 303–318.
- [8] U. Desideri, M. Antonelli, A simplified method for the evaluation of the performance of coal fired power plant with carbon capture, *Appl. Therm. Eng.* 64 (2014) 263–272.
- [9] R.S. Haszeldine, Carbon capture and storage: how green can black be? *Science* (80-) 325 (2009) 1647–1652.
- [10] A. Giuffrida, D. Bonalumi, G. Lozza, Amine-based post-combustion CO₂ capture in air-blown IGCC systems with cold and hot gas clean-up, *Appl. Energy*. 110 (2013) 44–54.
- [11] G. Zhao, B. Aziz, N. Hedin, Carbon dioxide adsorption on mesoporous silica surfaces containing amine-like motifs, *Appl. Energy*. 87 (2010) 2907–2913.
- [12] A.S. Kovvali, K.K. Sirkar, Carbon dioxide separation with novel solvents as liquid membranes, *Ind. Eng. Chem. Res.* 41 (2002) 2287–2295.
- [13] A. Hart, N. Gnanendran, Cryogenic CO₂ capture in natural gas, *Energy Procedia* 1 (2009) 697–706.
- [14] K. Fu, W. Rongwong, Z. Liang, Y. Na, R. Idem, P. Tontiwachwuthikul, Experimental analyses of mass transfer and heat transfer of post-combustion CO₂ absorption using hybrid solvent MEA-MeOH in an absorber, *Chem. Eng. J.* 260 (2015) 11–19, <https://doi.org/10.1016/j.cej.2018.09.030>.
- [15] B. Aghel, E. Heidaryan, S. Sahraie, S. Mir, Application of the microchannel reactor to carbon dioxide absorption, *J. Clean. Prod.* (2019).
- [16] B. Aghel, S. Sahraie, E. Heidaryan, K. Varmira, Experimental study of carbon dioxide absorption by mixed aqueous solutions of methyl diethanolamine (MDEA) and piperazine (PZ) in a microreactor, *Process Saf. Environ. Prot.* 131 (2019) 152–159.
- [17] M. Stec, A. Tatarczuk, L. Wieclaw-Solny, A. Krótki, M. Ściążko, S. Tokarski, Pilot plant results for advanced CO₂ capture process using amine scrubbing at the Jaworzno II Power Plant in Poland, *Fuel*. 151 (2015) 50–56.
- [18] J.M. Navaza, D. Gómez-Díaz, M.D. La Rubia, Removal process of CO₂ using MDEA aqueous solutions in a bubble column reactor, *Chem. Eng. J.* 146 (2009) 184–188.
- [19] T. Nittaya, P.L. Douglas, E. Croiset, L.A. Ricardez-Sandoval, Dynamic modelling and control of MEA absorption processes for CO₂ capture from power plants, *Fuel* 116 (2014) 672–691.
- [20] S.-Y. Oh, S. Yun, J.-K. Kim, Process integration and design for maximizing energy efficiency of a coal-fired power plant integrated with amine-based CO₂ capture process, *Appl. Energy*. 216 (2018) 311–322.
- [21] W. Ehrfeld, V. Hessel, H. Lowe, Modern microfabrication techniques for micro-reactors, *Microreactors New Technol. Mod. Chem.* (2000) 15–39.
- [22] C. Guangwen, Y. Jun, Y. Quan, Gas-liquid microreaction technology: recent developments and future challenges, *Chinese J. Chem. Eng.* 16 (2008) 663–669.
- [23] Y.E. Chunbo, C. Guangwen, Y. Quan, Process characteristics of CO₂ absorption by aqueous monoethanolamine in a microchannel reactor, *Chinese J. Chem. Eng.* 20 (2012) 111–119.
- [24] B. Aghel, E. Heidaryan, S. Sahraie, M. Nazari, Optimization of monoethanolamine for CO₂ absorption in a microchannel reactor, *J. CO₂ Util.* 28 (2018) 264–273.
- [25] A. Shooshtari, R. Kuzmicki, S. Dessiatoun, M. Alshehhi, E. Al Hajri, M.M. Ohadi, Enhancement of CO₂ absorption in aqueous diethanolamine amine using micro-channel contactors, *Carbon Manag. Technol. Conf., Carbon Management Technology Conference*, (2012).
- [26] C. Li, C. Zhu, Y. Ma, D. Liu, X. Gao, Experimental study on volumetric mass transfer coefficient of CO₂ absorption into MEA aqueous solution in a rectangular micro-channel reactor, *Int. J. Heat Mass Transf.* 78 (2014) 1055–1059.
- [27] X. Liu, J. Chen, X. Luo, M. Wang, H. Meng, Study on heat integration of supercritical coal-fired power plant with post-combustion CO₂ capture process through process simulation, *Fuel* 158 (2015) 625–633.
- [28] C.-C. Cormos, Economic evaluations of coal-based combustion and gasification power plants with post-combustion CO₂ capture using calcium looping cycle, *Energy* 78 (2014) 665–673.
- [29] M.R.M. Abu-Zahra, L.H.J. Schneiders, J.P.M. Niederer, P.H.M. Feron, G.F. Versteeg, CO₂ capture from power plants: Part I. A parametric study of the technical performance based on monoethanolamine, *Int. J. Greenh. Gas Control*. 1 (2007) 37–46.
- [30] P.F. Jahromi, J. Karimi-Sabet, Y. Amini, H. Fadaei, Pressure-driven liquid-liquid separation in Y-shaped microfluidic junctions, *Chem. Eng. J.* 328 (2017) 1075–1086.
- [31] S. Marsousi, J. Karimi-Sabet, M.A. Moosavian, Y. Amini, Liquid-liquid extraction of calcium using ionic liquids in spiral microfluidics, *AIChE J.* 356 (2019) 1467–1474, <https://doi.org/10.1016/j.cej.2018.09.030>.
- [32] A. Karimpour, A. D’Orazio, M.S. Shadloo, The effects of different nano particles of Al2O3 and Ag on the MHD nano fluid flow and heat transfer in a microchannel including slip velocity and temperature jump, *Phys. E Low-Dimensional Syst. Nanostruct.* 86 (2017) 146–153.
- [33] M.R. Safaei, M. Gooarzi, O.A. Akbari, M.S. Shadloo, M. Dahari, Performance evaluation of nanofluids in an inclined ribbed microchannel for electronic cooling applications, *Electron. Cool.* 832 (2016).
- [34] M.Y.A. Jamalabadi, M. DaqiqShirazi, A. Kosar, M.S. Shadloo, Effect of injection angle, density ratio, and viscosity on droplet formation in a microfluidic T-junction, *Theor. Appl. Mech. Lett.* 7 (2017) 243–251.
- [35] D.T. Nguyen, A.P. Esser-Kahn, A microvascular system for chemical reactions using surface waste heat, *Angew. Chemie Int. Ed.* 52 (2013) 13731–13734.
- [36] H. Liu, C. Yao, Y. Zhao, G. Chen, Desorption of carbon dioxide from aqueous MDEA solution in a microchannel reactor, *Chem. Eng. J.* 307 (2017) 776–784.
- [37] H. Liu, C. Yao, Y. Zhao, G. Chen, Heat transfer characteristics of CO₂ desorption from N-methyldiethanolamine solution in a microchannel reactor, *Chem. Eng. Technol.* 41 (2018) 1398–1405.
- [38] A.-K. Kunze, P. Lutze, M. Kopatschek, J.F.J. Maćkowiak, M. Grünwald, A. Górk, Mass transfer measurements in absorption and desorption: Determination of mass transfer parameters, *Chem. Eng. Res. Des.* 104 (2015) 440–452.
- [39] H. Kierzkowska-Pawlak, A. Chacuk, Kinetics of CO₂ desorption from aqueous N-methyldiethanolamine solutions, *Chem. Eng. J.* 168 (2011) 367–375.
- [40] R.H. Weiland, N.A. Hatcher, J.L. Nava, Post-combustion CO₂ capture with amino-acid salts, *Pap. Present. GPA Eur. Meet.* 2010, p. 24.
- [41] U. Arachchige, N. Aryal, D.A. Eimer, M.C. Melaen, Viscosities of pure and aqueous solutions of monoethanolamine (MEA), diethanolamine (DEA) and N-methyl-diethanolamine (MDEA), *Annu. Trans. Nord. Rheol. Soc.* 21 (2013) 299–306.
- [42] X. Chen, Carbon dioxide thermodynamics, kinetics, and mass transfer in aqueous piperazine derivatives and other amines (2011).
- [43] R.U. Owolabi, M.A. Usman, A.J. Kehinde, Modelling and optimization of process variables for the solution polymerization of styrene using response surface methodology, *J. King Saud. Univ. Sci.* 30 (2018) 22–30.
- [44] Z.N. Garba, I. Bello, A. Galadima, A.Y. Lawal, Optimization of adsorption conditions using central composite design for the removal of copper (II) and lead (II) by defatted papaya seed, *Karbala Int. J. Mod. Sci.* 2 (2016) 20–28.
- [45] M. Mourabet, A. El Rhilassi, H. El Boujaady, M. Bennani-Ziatni, A. Taitai, Use of response surface methodology for optimization of fluoride adsorption in an aqueous solution by Brushite, *Arab. J. Chem.* 10 (2017) S3292–S3302.
- [46] E. Heidaryan, A note on model selection based on the percentage of accuracy-precision, *J. Energy Resour. Technol.* 141 (2018), <https://doi.org/10.1115/1.4041844>.
- [47] D.C. Montgomery, Y. Tanawannapong, A. Kaewchada, A. Jaree, V.B. Veljković, M.O. Biberdžić, I.B. Banković-Ilić, I.G. Djalović, M.B. Tasić, Z.B. Nježić, O.S. Stamenković, Design and analysis of experiments, John Wiley & Sons, Limited, 2019.
- [48] J. Gao, J. Yin, F. Zhu, X. Chen, M. Tong, W. Kang, Y. Zhou, J. Lu, Integration study of a hybrid solvent MEA-Methanol for post combustion carbon dioxide capture in packed bed absorption and regeneration columns, *Sep. Purif. Technol.* 167 (2016)

- 17–23.
- [49] M.R.M. Abu-Zahra, J.P.M. Niederer, P.H.M. Feron, G.F. Versteeg, CO₂ capture from power plants: Part II. A parametric study of the economical performance based on mono-ethanolamine, *Int. J. Greenh. Gas Control.* 1 (2007) 135–142.
- [50] X. Zhang, K. Fu, Z. Liang, W. Rongwong, Z. Yang, R. Idem, P. Tontiwachwuthikul, Experimental studies of regeneration heat duty for CO₂ desorption from diethylenetriamine (DETA) solution in a stripper column packed with Dixon ring random packing, *Fuel* 136 (2014) 261–267.
- [51] X. Li, S. Wang, C. Chen, Experimental study of energy requirement of CO₂ desorption from rich solvent, *Energy Procedia* 37 (2013) 1836–1843.
- [52] S. Sahraie, H. Rashidi, P. Valeh-e-Sheyda, An optimization framework to investigate the CO₂ capture performance by MEA: Experimental and statistical studies using Box-Behnken design, *Process Saf. Environ. Prot.* 122 (2019) 161–168.
- [53] P. Galindo, A. Schäffer, K. Brechtel, S. Unterberger, G. Scheffknecht, Experimental research on the performance of CO₂-loaded solutions of MEA and DEA at regeneration conditions, *Fuel*. 101 (2012) 2–8.